

# A De Novo Mutation in *TEAD1* Causes Non-X-Linked Aicardi Syndrome

Isabelle Schrauwen,<sup>1-3</sup> Szabolcs Szelinger,<sup>1,2</sup> Ashley L. Siniard,<sup>1,2</sup> Jason J. Corneveaux,<sup>1,2</sup> Ahmet Kurdoglu,<sup>1,2</sup> Ryan Richholt,<sup>1,2</sup> Matt De Both,<sup>1,2</sup> Ivana Malenica,<sup>1,2</sup> Shanker Swaminathan,<sup>1,2</sup> Sampathkumar Rangasamy,<sup>1,2</sup> Neil Kulkarni,<sup>4</sup> Saunder Bernes,<sup>4</sup> Jeffrey Buchhalter,<sup>5</sup> Keri Ramsey,<sup>1,2</sup> David W. Craig,<sup>1,2</sup> Vinodh Narayanan,<sup>1,2</sup> and Matthew J. Huentelman<sup>1,2</sup>

<sup>1</sup>Dorrance Center for Rare Childhood Disorders, Translational Genomics Research Institute, Phoenix, Arizona, United States

<sup>2</sup>Neurogenomics Division, Translational Genomics Research Institute, Phoenix, Arizona, United States

<sup>3</sup>Department of Medical Genetics, University of Antwerp, Antwerp, Belgium

<sup>4</sup>Phoenix Children's Hospital, Phoenix, Arizona, United States

<sup>5</sup>Alberta Children's Hospital, University of Calgary, Alberta, Canada

Correspondence: Matthew J. Huentelman, The Translational Genomics Research Institute (TGen), 445 N 5th Street, Phoenix, AZ 85004, USA; mhuentelman@tgen.org.

Submitted: December 15, 2014

Accepted: April 8, 2015

Citation: Schrauwen I, Szelinger S, Siniard AL, et al. A de novo mutation in *TEAD1* causes non-X-linked Aicardi syndrome. *Invest Ophthalmol Vis Sci.* 2015;56:3896-3904. DOI:10.1167/iov.14-16261

**PURPOSE.** Aicardi syndrome (AIC) is a congenital neurodevelopmental disorder characterized by infantile spasms, agenesis of the corpus callosum, and chorioretinal lacunae. Variation in phenotype and disease severity is well documented, but chorioretinal lacunae represent the most constant pathological feature. Aicardi syndrome is believed to be an X-linked-dominant disorder occurring almost exclusively in females, although 46, XY males with AIC have been described. The purpose of this study is to identify genetic factors and pathways involved in AIC.

**METHODS.** We performed exome/genome sequencing of 10 children diagnosed with AIC and their parents and performed RNA sequencing on blood samples from nine cases, their parents, and unrelated controls.

**RESULTS.** We identified a de novo mutation in autosomal gene *TEAD1*, expressed in the retina and brain, in a patient with AIC. Mutations in *TEAD1* have previously been associated with Sveinsson's chorioretinal atrophy, characterized by chorioretinal degeneration. This demonstrates that *TEAD1* mutations can lead to different chorioretinal complications. In addition, we found that altered expression of genes associated with synaptic plasticity, neuronal development, retinal development, and cell cycle control/apoptosis is an important underlying potential pathogenic mechanism shared among cases. Last, we found a case with skewed X inactivation, supporting the idea that nonrandom X inactivation might be important in AIC.

**CONCLUSIONS.** We expand the phenotype of *TEAD1* mutations, demonstrate its importance in chorioretinal complications, and propose the first putative pathogenic mechanisms underlying AIC. Our data suggest that AIC is a genetically heterogeneous disease and is not restricted to the X chromosome, and that *TEAD1* mutations may be present in male patients.

**Keywords:** Aicardi, retinal lacunae, *TEAD1*, X-linked, seizure

Aicardi syndrome (AIC) is a rare neurodevelopmental disorder characterized by a classic triad of symptoms including infantile spasms, agenesis of the corpus callosum, and chorioretinal lacunae.<sup>1</sup> However, the clinical presentation of AIC seems much broader, with a wide range in severity of these classic symptoms and the presence of additional phenotypic characteristics. Aicardi reported that no feature except chorioretinal lacunae is constant. Other anomalies include mental retardation, abnormal vertebrae, asymmetry of the cerebral hemispheres, cerebellar hypoplasia, dilated cerebral ventricles, neuronal migration disturbances (heterotopia, polymicrogyria), and cysts of the posterior fossa and choroid plexus. Although the ophthalmic hallmark and defining feature of AIC is the cluster of distinctive chorioretinal lacunae surrounding the optic nerve(s), the spectrum of ocular,

papillary, and retinal anomalies also varies widely, from nearly normal to dysplasia of the optic nerve and to severe microphthalmos.<sup>2</sup> Other findings include retinal dysplasia, optic nerve dysplasia, colobomas of the optic nerve and choroid, microphthalmia, persistent pupillary membrane, and glial tissue extending from the disc.<sup>3,4</sup> The outcome of AIC is usually severe, with a high early mortality, considerable morbidity, and a generally poor developmental outcome.<sup>1</sup> The incidence in the United States is 1 per 105,000.<sup>5</sup>

Aicardi syndrome occurs almost exclusively in females. The occurrence of AIC in males is rare, but reports have shown that XXY males with AIC exist.<sup>6,7</sup> There have been several reports of AIC cases with cytogenetic alterations at Xp22.<sup>8,9</sup> Based on the clinical and cytogenetic data, the inheritance pattern of AIC was thought to be X-linked dominant with early embryonic

TABLE. Phenotypic Characteristics of the 10 AIC Cases Included in This Study

Family Number	Gene	Sequenced	Corpus Callosum	Eye	Infantile Seizures	Other
Family 1		P, M, F	Agenesis	Retinal lacunae	At 3 mo	Prenatal cysts, hydrocephalus
Family 2	<i>TEAD1</i>	P, M, F	Normal	Retinal lacunae	At 3.5 mo	Cerebellar cyst, periventricular heterotopias
Family 3		P, M, F	Agenesis	Retinal lacunae	At 10 wk	Enlarged III IV ventricles, hydrocephalus, no walking or talking
Family 4		P, M, F	Complete or partial agenesis	Retinal lacunae	At 10 wk	
Family 5		P, M, F	Agenesis	Bilateral optic nerve colobomas, bilateral retinal lacunae, and microphthalmia	At 3.5 mo	
Family 6		P, M	Partial agenesis	Retinal lacunae	At 6 wk	
Family 7	<i>OCELI</i>	P, M, F	Small remnant	Retinal lacunae	At 3 mo	Postfossa arachnoid cyst
Family 8		P, M, F	Agenesis	Retinal lacunae	At 10 wk	Global developmental delay; heterotopic gray matter, frontal lobes; intracranial cysts; ventricular dilatation ex vacuo; and abnormal sulcation pattern, failure to thrive, trunkal hypotonia, scoliosis with trunkal curvature, babbles, dental caries
Family 9		P, M, F	Almost entirely preserved	Retinal lacunae 1 eye	At 3 mo	Cysts in brain
Family 10		P, M	Agenesis	Retinal lacunae left eye, mild	At 3 mo	

P, proband; M, mother; F, father.

lethality in hemizygous males. As affected females have never been known to reproduce and multiple affected relatives have not been reported, all cases are thought to represent new mutations,<sup>9</sup> in particular, de novo germline mutations inherited from the father.<sup>10</sup> The AIC locus mapped to Xp22<sup>8,9</sup> is suggestive,<sup>1</sup> and no AIC gene has been identified to date.

More recently, two cases of AIC in 46, XY males have been described.<sup>11,12</sup> This suggests that non-X-linked types of AIC do exist and supports the idea of genetic heterogeneity. The preponderance in females indicates that non-X-linked genes might cause only a small fraction of AIC, or that because of the typical differential diagnostic approach to AIC, males with the disease are present in the population but carry a different diagnosis.

In this study, we investigated 10 girls with a diagnosis of AIC and their parents by exome or genome sequencing. In one case, we identified a de novo mutation in an autosomal gene, previously linked to eye and vision function. This supports the hypothesis of genetic heterogeneity and the potential for non-X-linked cases of the disease.

## MATERIALS AND METHODS

### Patient Enrollment

The participating families provided written consent and were enrolled into a research study at the Dorrance Center for Rare Childhood Disorders at the Translational Genomics Research Institute (TGen). Cases with AIC were referred by clinical neurologists or via an AIC family network, and all patients were examined by a pediatric neurologist and ophthalmologist. Aicardi syndrome is considered in young girls when infantile spasms are present. The diagnosis of AIC was confirmed by an exam that consisted of a neurological examination including

brain magnetic resonance imaging (MRI) and a detailed ophthalmologic exam including fundus photography. The presence of three classic features, infantile spasms, complete or partial agenesis of the corpus callosum, and chorioretinal lacunae, is diagnostic for AIC. There is a great variety in severity, however,<sup>13</sup> and corpus callosum agenesis is not the hallmark of the disease and is not even necessary for diagnosis if other cerebral pathologies, such as cysts, are present.<sup>1</sup> Eight cases in our study show the classic triad of AIC, with a partial or complete agenesis of the corpus callosum (Table). Two cases had a completely intact corpus callosum but displayed other features (cysts in the cerebellum) in addition to chorioretinal lacunae and infantile spasms. The study protocol and consent procedure were approved by the Western Institutional Review Board (WIRB), and the research followed the tenets of the Declaration of Helsinki.

### Exome/Genome Sequencing

All families were analyzed by exome sequencing except for families 2 and 3, who were sequenced using a whole-genome sequencing approach. Family 1 was sequenced with both exome and whole-genome sequencing. Libraries were prepared with Illumina's Truseq DNA Sample Preparation Kit (Illumina, Inc., San Diego, CA, USA), following the manufacturer's protocol. For exome sequencing, an extra step of exome enrichment was included (Truseq exome enrichment kit; Illumina, Inc.). Sequencing was done by 100-bp paired-end sequencing on a HiSeq2000 or HiSeq2500 instrument (Illumina, Inc.).

### RNA Sequencing (RNA-seq)

Blood was collected into PAXgene tubes (Qiagen, Venlo, The Netherlands) from nine AIC cases (average age = 8) and 15 of

their parents (average age = 40; Table), with the exception of family 2. In addition, RNA was available from four other children through the Center for Rare Childhood Disorders (average age = 11) to provide an age-matched control set. These children either were healthy and had no signs of disease or presented with completely different features than AIC (i.e., migraine, hypotonia, Crisponi syndrome). RNA extraction was done using the PAXgene blood RNA kit (Qiagen). RNA was prepared for sequencing using Illumina's Truseq RNA Sample Preparation Kit, followed by 50-bp paired-end sequencing on a HiSeq2000 or HiSeq2500 instrument (Illumina, Inc.).

### Data Analysis

For DNA sequencing, reads were aligned to the Human Genome (Hg19/GRC37) using Burrows-Wheeler transform alignment (BWA v.0.7.5).<sup>14</sup> Next, PCR duplicates were removed using Picard v1.92,<sup>15</sup> and base quality recalibration, indel realignment and single nucleotide polymorphism (SNP) and indel discovery were performed using the Genome analysis toolkit (GATK v2.5-2).<sup>16</sup> Last, data were filtered against dbSNP137, 1000 Genomes, and an in-house exome SNP database and then annotated with SnpEff 3.2a.<sup>17</sup>

For RNA sequencing, reads were aligned to the Human Genome (GRC37.74) using RNASTAR\_2.3.1.<sup>18</sup> Read counts were generated using HTSeq v0.6.1<sup>19</sup> and differential expression was calculated using Deseq2.<sup>20</sup> Only genes that were significant and with fold change in the same direction compared to both the parent and age-matched control group were investigated further. Fragments per kilobase of exon per million fragments mapped (FPKM) were calculated using Cufflinks,<sup>21</sup> and plots were generated using Ggplot2 (R v3.0.3). Genes were selected that were significant adjusted for multiple testing compared to one control group<sup>20</sup> and nominally significant in the other. Next, low-expressed genes were excluded (minimum FPKM > 0.7 in either group). Genes were then annotated using BioMart (Ensembl, Hinxton, Cambridgeshire, UK) and ribosomal, globin genes, pseudogenes, and X or Y chromosome genes were removed. Only protein coding and noncoding RNAs were retained. Last, important neuronal/retinal genes and pathways were identified using Reactome<sup>22</sup> and ToppGene Suite for gene list enrichment analysis and candidate gene prioritization.<sup>23</sup>

### Expression Profiling

Thirty-six different human tissues were collected for expression profiling. Total RNA for 32 tissues was purchased at Asterand (Detroit, MI, USA), and inner ear tissues were collected by translabyrinthine and transcochlear approaches to tumors of the skull base as part of a different study. RNA was extracted using TRIzol (Life Technologies, Carlsbad, CA, USA). Samples were prepped and sequenced as mentioned earlier. Reads were aligned with TopHat2 to GRC37.74, which utilizes Bowtie2.<sup>24</sup> FPKM values were calculated using Cufflinks v2.1.1.<sup>21</sup> Ggplot2 (R v3.0.3) was used to visualize output.

### X-Inactivation Ratio

We determined the X-chromosome inactivation (XCI) ratio in nine AIC patients using allelic expression data from RNA-seq data.<sup>25</sup> In three of the nine patients, the XCI ratio was also measured using the standard human androgen receptor (HUMARA) methylation assay.<sup>26</sup> Sequenced reads were aligned to the Human Genome using Bowtie2,<sup>27</sup> and at each position across the X chromosome the number of reads was obtained.<sup>15</sup> The allelic ratio was then estimated at each heterozygous locus. Next, the SNPs were further filtered by the following criteria: (1) SNPs within the PAR1 and PAR2 pseudoautosomal regions were excluded as they follow autosomal inheritance;

(2) only high-confidence variants (filter score of PASS by GATK) were kept; (3) all loci without a dbSNP identifier were excluded; and (4) a minimum 20× sequence coverage was necessary. After fitting the allelic ratio for these SNPs to a semiparametric model,<sup>28</sup> we obtained the XCI ratio for each AIC patient ( $n = 9$ ).<sup>25</sup>

### Sanger Sequencing

Polymerase chain reaction (PCR) was carried out under standard conditions. Direct sequencing of the PCR product was performed on an ABI3130XL sequencer (Applied Biosystems, Inc., Foster City, CA, USA).

## RESULTS

### Clinical Features

An overview of the clinical features of all 10 families investigated in this study is presented in the Table. More detailed characteristics are listed here for family 2, in whom a mutation in *TEAD1* was discovered (Fig. 1).

Family 2: This 5.5-year-old girl has two unaffected siblings. Prenatal ultrasound at 30 weeks gestation suggested a cyst in the brain, which was confirmed by a prenatal MRI. She was delivered by Cesarean section at 39 weeks gestation. Head ultrasound and rapid sequence limited MRI study done a few days after birth showed a midline posterior fossa cyst, periventricular heterotopias, and a normal corpus callosum. At 3.5 months, she developed infantile spasms. Visual assessment of the eye revealed a normal sclera, cornea, anterior chamber, uveal tract, lens, and a clear vitreous fluid. She could not fix and follow an object. The cycloplegic refraction was -1.50 diopters (D) for both eyes, indicating (mild) myopia. The patient has difficulty recognizing faces and viewing fine labels. A fundus photograph showed retinal lacunae (4.5 months of age), supporting a clinical diagnosis of AIC (Fig. 1). She crawls, pulls to stand, and cruises around furniture; makes noises; knows the sign for "eat" and eats solid food by mouth. She is nearsighted.

Detailed characteristics for family 7 can be found in Figure 1 and the Supplementary Material (Supplementary Clinical Information 1).

### Sequencing

Exome and/or genome sequencing in 10 trios with affected children with AIC identified significant variants in two families:

In family 2, we identified a de novo nonsense mutation in *TEAD1* (Chr11: 12904591G>A; NM\_021961.5:c.618G>A; NP\_068780.2:p.Trp206Ter). In family 7, we identified a de novo nonsynonymous variant in *OCELI1* (Chr19:17338695G>A; NM\_024578.1:c.499G>A; NP\_078854.1:p.Ala167Thr). Neither of these variants was present in the 1000 Genomes or dbSNP database or in our in-house exome database (116 exomes). The mutation in *OCELI1* was damaging according to MutationTaster (<http://www.mutationtaster.org/> [in the public domain]), likelihood ratio test (LTR; [http://www.genetics.wustl.edu/jflab/lrt\\_query.html](http://www.genetics.wustl.edu/jflab/lrt_query.html) [in the public domain]), and Polyphen2 (<http://genetics.bwh.harvard.edu/pph2/> [in the public domain]), and affects a highly conserved residue (PhyloP = 2.1). p.Ala167Thr (*OCELI1*) has been seen once in 121328 exomes, p.Trp206Ter (*TEAD1*) has not been reported in 121328 exomes (Exome Aggregation Consortium [ExAC]; <http://exac.broadinstitute.org> [in the public domain]). Combined Annotation Dependent Depletion (CADD) scores for the *TEAD1* and *OCELI1* variant are, respectively, 40 and 15.3.<sup>29</sup> Sanger sequencing in each trio confirmed the presence and inheritance of these variants. In

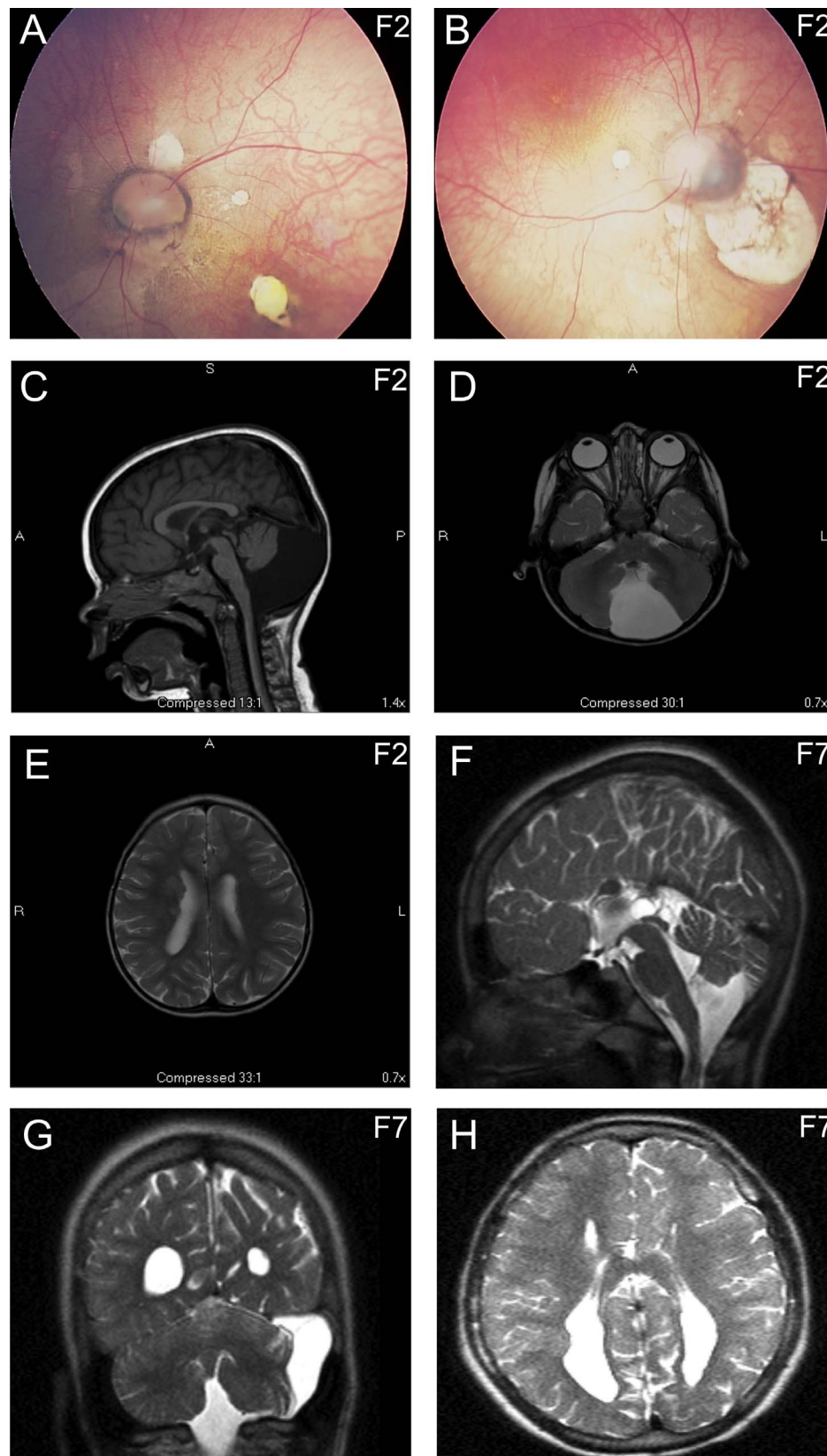


**FIGURE 1.** Pictures from the patients from family 2 (*TEAD1*) and family 7 (*OCELI*). (A–E) Family 2 *TEAD1* case, showing chorioretinal lacunae and an intact corpus callosum (brain MRI images at 27 months). (A) Left eye fundus photograph shows a peripapillary lacuna and two separate retinal lacunae. (B) Right eye fundus photograph showing multiple peripapillary lacunae. (C) Midsagittal T1 image demonstrating an intact corpus callosum, a large posterior fossa cyst, and posterior rotation of the cerebellar vermis. (D) Axial T2 image showing a midline posterior fossa cyst. (E) Axial T2 image of the brain showing right frontal periventricular heterotopias. (F–H) Pictures from AIC case family 7 (*OCELI*). (F) 1-bang MRI at 12.5 years of age; sagittal T2 image shows presence of the genu of the corpus callosum, but absence of the body and splenium. (G) Coronal T2 image shows a posterior fossa arachnoid cyst. (H) Colpocephaly, ventricular configuration typical of agenesis of corpus callosum (axial T2). F2, AIC case family 2; F7, AIC case family 7.

the other eight families, only variants of unknown significance were identified.

### RNA-Seq

To identify possible disease mechanisms shared among AIC cases, we compared gene expression in nine AIC cases (excluding family 2 with the *TEAD1* mutation) to their parents and an age-matched control group. This identified 147 genes that are significantly different between cases and the two comparison groups (Supplementary Table S1; Supplementary Fig. S1). One hundred forty-two were protein coding and five were noncoding RNAs. Some of the pathways that were significantly represented in this gene set included E2F-mediated regulation of DNA replication ( $P = 0.002$ ; ID 105778) and the cell cycle ( $P = 0.002$ ; ID 530733). The three most significantly differentially expressed genes for both groups are *AP3B2* ( $P_{\text{adj\_parents}} = 2.09 \times 10^{-14}$ ;  $P_{\text{adj\_controls}} = 5.87 \times 10^{-16}$ ), *ASIC1* ( $P_{\text{adj\_parents}} = 2.22 \times 10^{-10}$ ;  $P_{\text{adj\_controls}} = 4.81 \times 10^{-3}$ ), and *GRIK5* ( $P_{\text{adj\_parents}} = 1.14 \times 10^{-7}$ ;  $P_{\text{adj\_controls}} = 3.11 \times 10^{-3}$ ), which all play an important role in brain development, neuronal plasticity, and seizures. *ASIC1* is also important in retinal biology.<sup>30</sup> Eighteen genes were found that are important in either brain development or the development of the eye. More specifically, neuronal genes either are important in synaptic plasticity (*GRIK5*, *ASIC1*, *IFT57* [interacts with *HOMER1*], *SVA2*, *HTRA3*, *CAMKK1*, *PTGS2*, *AP3B2*, and *ABAT*) or have previously been reported to be implicated in seizures (*GRIK5*, *ASIC1*, *SVA2*, *HTRA3*, *PTGS2*, *KCNE1*, *AP3B2*, *ABAT*, and *GIPC3*) (Fig. 2; Supplementary Figs. S2, S3). Three more genes not listed in Figure 2 are important in neuronal development: *FGD4*, *KIAA1324*, and *LRN3*. Several genes important in eye/retina development are also differentially expressed in AIC as compared to controls: *NEK2*, *LRP5*, *CDK1*, *PTGS2*, *ASIC1*, *IFT57*, and *GPX3* (Fig. 2; Supplementary Figs. S2, S3). Of interest might be *GEMIN2*, important in the development of the corpus callosum, which is upregulated in AIC cases; however, this gene reaches only nominal significance when compared to both control groups.

Lastly, as *TEAD1* has an important function in the control of cellular growth and apoptosis, we also looked for genes involved in cell cycle control and apoptosis (Fig. 3). We found 18 genes important in cell cycle control that were dysregulated in our cases (Fig. 3A). Three genes are involved in apoptosis: proapoptotic *DAPK2* is downregulated, and antiapoptotic *BIRC5* and proapoptotic *CD27* are upregulated (Fig. 3B). We could not find any significant dysregulation in any genes of the Hippo pathway. *DCHS1*, however (Hippo signaling), was upregulated in cases versus parents ( $P = 2.74 \times 10^{-7}$ ) and shows a trend toward significance when compared to the age-matched controls ( $P = 0.09$ ). *TEAD1* mRNA is expressed at a very low level in blood (FPKM  $\sim 1$ ), and no statistical difference was found between the nine other AIC cases and both control groups, although this is likely due to its low expression level.

### X-Inactivation Ratio

We determined the XCI ratio in nine AIC patients using allelic expression data from RNA-seq data (Fig. 2; Supplementary Table S2)<sup>25</sup> and also obtained the XCI ratio of three patients using the standard HUMARA methylation test. One of the AIC cases showed extremely skewed X inactivation with an XCI ratio of 90:4 (family 10, Fig. 4). None of the other cases reached the threshold for moderately skewed XCI (80:20); however, the case from family 3 reaches this threshold with the HUMARA assay (83:17). This suggests that the AIC case from family 10 and possibly also the case from family 3 have a causal mutation or defect located on the X chromosome.

### Expression Profiling of *TEAD1*

We performed expression profiling of *TEAD1* and *OCELI1* across 36 different human tissues using RNA-seq. We found that both genes are highly expressed in the brain (Supplementary Fig. S4) and various other tissues.

### DISCUSSION

This study investigated 10 cases of AIC by exome/genome sequencing to identify the pathogenic mechanisms that lead to disease (Table). Eight cases in our study show the classic triad of AIC, with a partial or complete agenesis of the corpus callosum (Table). There is a great variation in severity, however, and corpus callosum agenesis is not the hallmark of the disease and is not necessary for diagnosis if other cerebral pathologies, such as cysts, are present.<sup>1</sup> Two cases had a completely intact corpus callosum but displayed other features (cysts in the cerebellum) in addition to chorioretinal lacunae and infantile spasms.

Sequencing revealed a family with a de novo mutation in an autosomal gene, *TEAD1*, that leads to a premature truncation of the protein (p.Trp206Ter). The Tea domain family member (TEAD) proteins, or transcription enhancer factors (TEFs), comprise a conserved family of eukaryotic DNA-binding proteins that regulate expression of multiple genes.<sup>31</sup> A nonsynonymous mutation in the *TEAD1* gene, p.Y421H, has previously been found in a large Icelandic pedigree with Sveinsson's chorioretinal atrophy, also referred to as helicoid peripapillary chorioretinal degeneration or atrophía areata. This is an autosomal dominant eye disease characterized by symmetrical lesions radiating from the optic disc involving the retina and the choroid.<sup>32</sup> A missense mutation corresponding to human Y421H in mouse *Tead1* (Y410H) showed that the mutation reduced the ability of *Tead1* to interact with its cofactors Yap (YES-associated protein) and Taz (transcriptional coactivator with PDZ-binding motif) and abolished the transcriptional activity of *Tead1* when it was coexpressed with Yap or Taz.<sup>33</sup> Although Y410H shows reduced ability to interact with YAP,<sup>33</sup> the antiapoptotic ability of overexpressed mutant *TEAD1* compared to wild-type through the upregulation of *Livin* has not been affected.<sup>34</sup> In contrast to this, our patient has a nonsense mutation (p.Trp206Ter), which leads to a complete loss of function. A partially (and selective) active *TEAD1* in Sveinsson's chorioretinal atrophy (SCRA), compared to a full loss of *TEAD1* in AIC, could explain differences in the type of retinal lesions, which are more organized in AIC, and the additional symptoms including infantile spasms, cerebellar cyst, and periventricular heterotopias in our AIC patient. *YAPI* gene defects are associated with ocular coloboma, hearing impairment, cleft lip/palate, learning difficulties, and hematuria.<sup>35</sup> All these symptoms have been associated with AIC as well, with the exception of hematuria. This suggests that perhaps other Aicardi patients may have mutations within the Hippo pathway.

The Hippo pathway is a highly conserved signaling pathway that has been identified as a key molecular mechanism for governing organ size regulation and regulates cell number by modulating cell proliferation, cell death, and cell differentiation.<sup>36</sup> Yap and *TEAD1* are both components of the Hippo pathway, and *TEAD* is the key transcription factor in the Hippo pathway acting downstream from YAP.<sup>37</sup> The core Hippo pathway was described initially in *Drosophila* and is largely conserved in vertebrates and mammals. It alters gene expression in response to changes in cell shape, adhesion, and density.<sup>38</sup> In addition to the regulation of cell proliferation, *TEAD1* is also important in the regulation of apoptosis. The apoptotic resistance conferred by altered *TEAD1* expression is mediated by the transcriptional upregulation of *Livin*, a member of the inhibitor of apoptosis protein (IAP) family.<sup>34</sup>

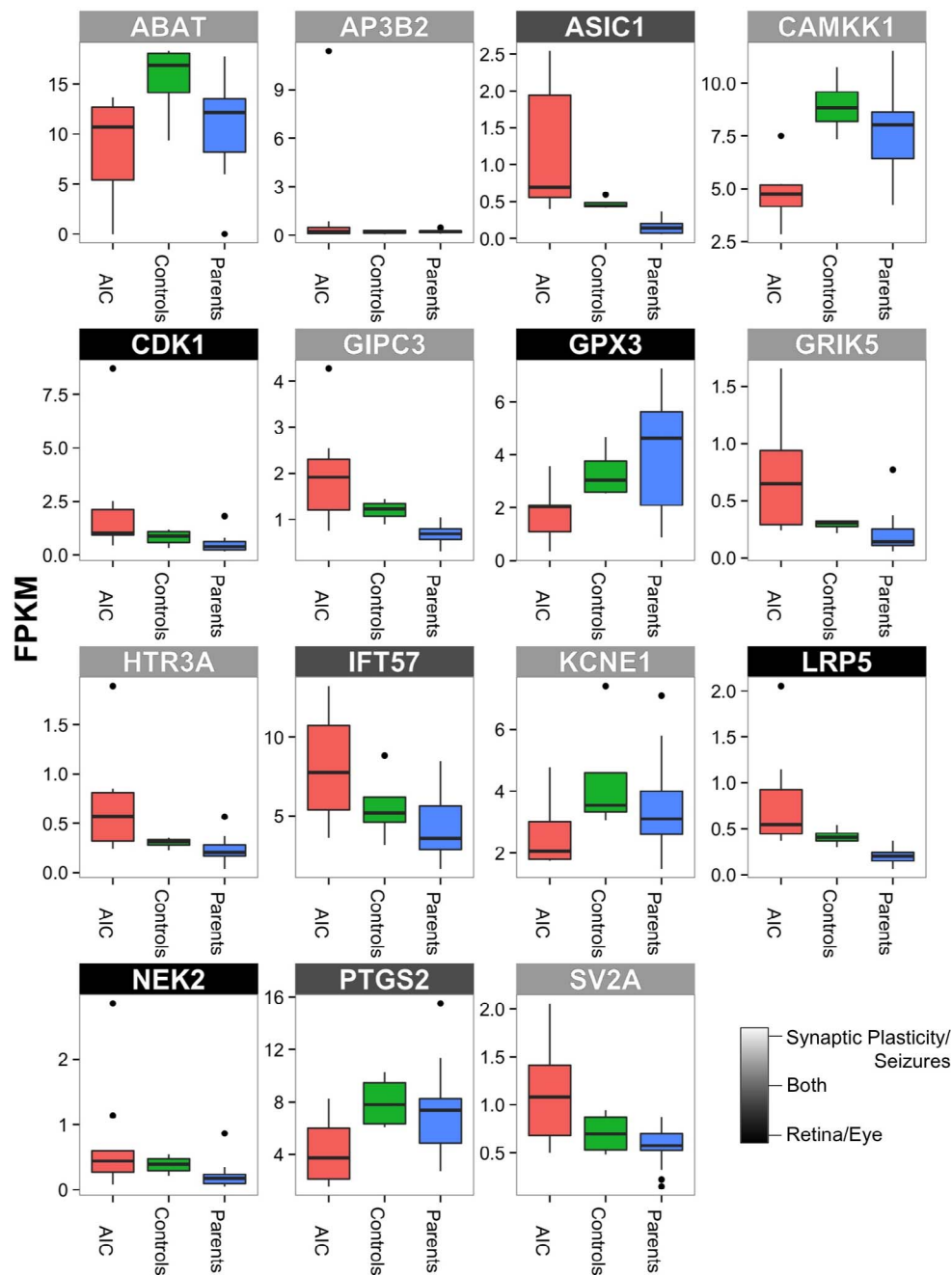


**FIGURE 2.** Box plots showing the most significant dysregulated genes identified by RNA-seq in AIC cases compared to two sets of controls: parents and age-matched controls. Genes presented here are important in retinal development and neuronal plasticity or are seizure associated. Note that for *AP3B2*, the association is significant due to an extreme upregulation in family 10 and to a lesser extent in family 7, which might suggest a shared pathway unique to these cases.

Overexpression of mutant *TEAD1* (Y421H) implicated in SCRA that strongly reduces its interaction with YAP can induce Livin expression and protect cells from induced apoptosis, suggesting that YAP is not the cofactor involved in Livin repression.<sup>34</sup> Moreover, TEA domain protein 1 (*TEAD1*) is able to positively activate the transcription of *NAIP*, neuronal apoptosis inhibitory protein, an inhibitor of apoptosis,<sup>39</sup> and interaction of *TEAD1* with YAP is required for *NAIP* upregulation.

The previous association of *TEAD1* mutations with peripapillary retinal lesions<sup>32</sup> confirms the neurological and retinal importance of this gene during development. *TEAD1* is important in cell growth, proliferation, and apoptosis. Selective

dysregulation in tissues that express high levels of *TEAD1* during development might explain the specific targeted lesions. Indeed, spatial expression analysis in *Xenopus laevis* during embryonic development showed that the *TEAD1* mRNAs were predominantly detected in the eye and secondly in the somites and brain. Other tissues include the heart and otic vesicle, the anterior part of the neural tube.<sup>40</sup> This eye and brain “dominant” expression during development may contribute to the region-specific developmental defects. We also performed an extensive expression profiling of *TEAD1* across multiple human tissues (Supplementary Fig. S5). We found that it is highly expressed in several tissues, including the inner ear,

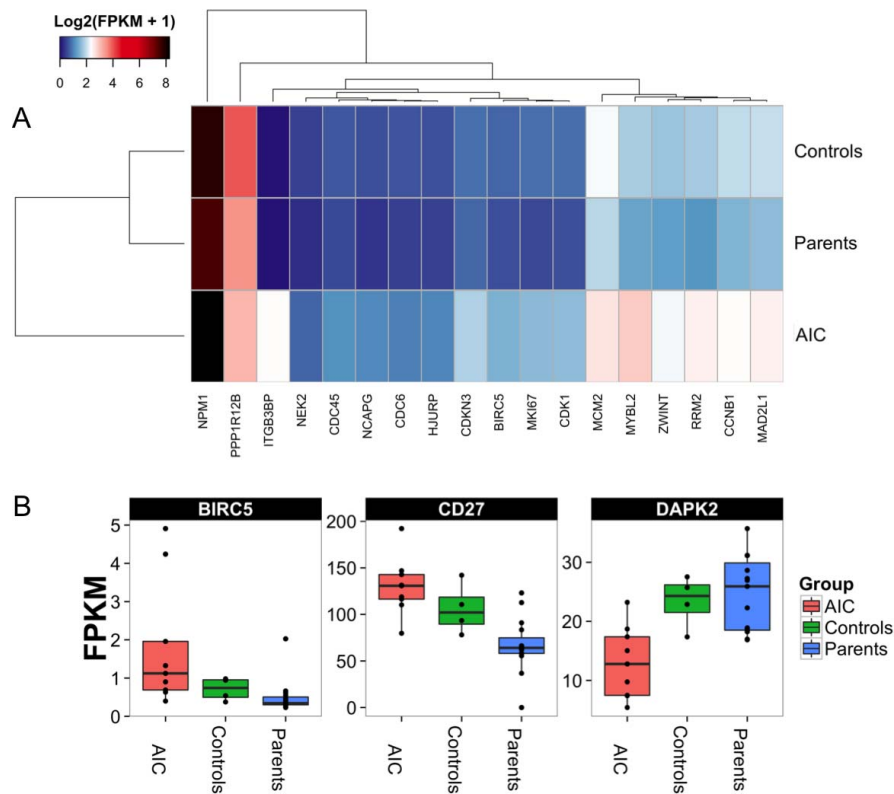


**FIGURE 3.** Genes involved in cell cycle control (A) and apoptosis (B) significantly dysregulated in patients with AIC syndrome compared to two sets of controls: parents and age-matched controls. The box plot shows the median and the first and third quartiles (the 25th and 75th percentiles) per group.

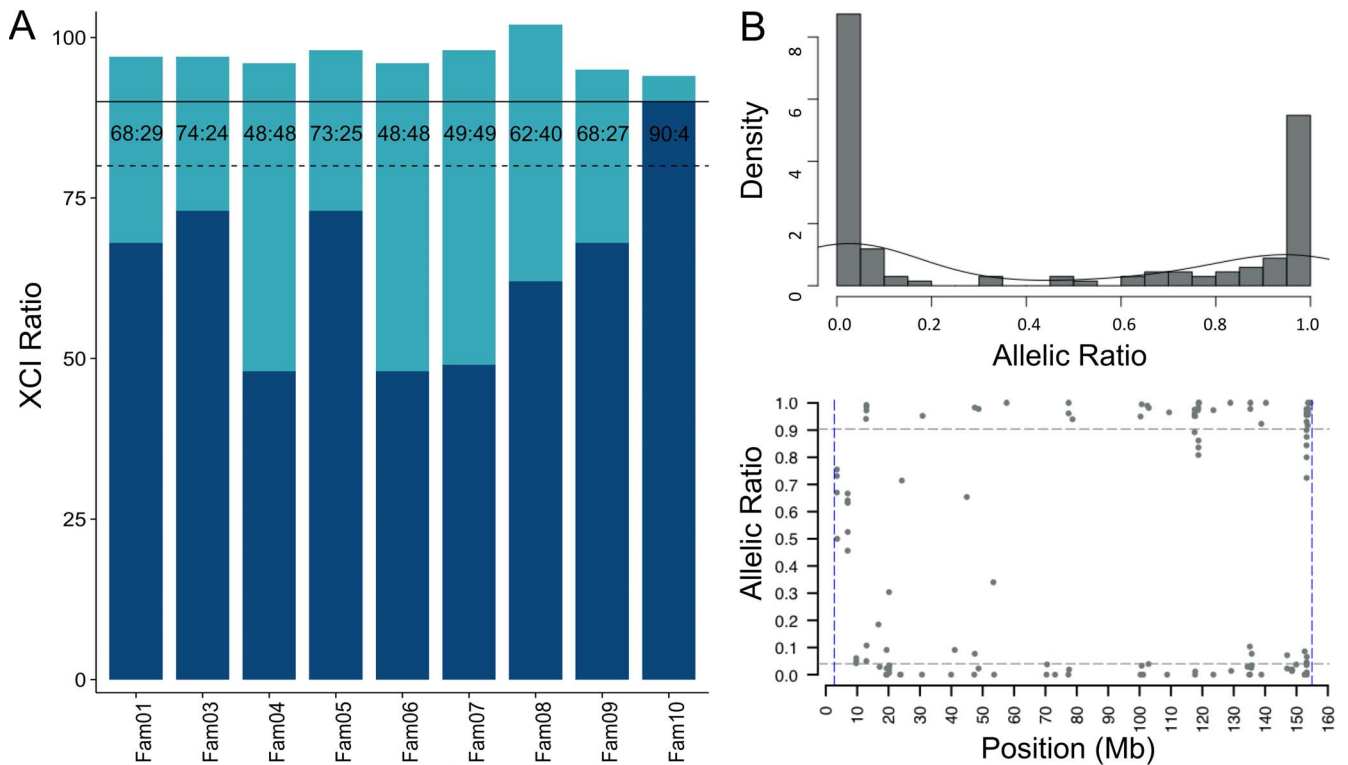


**FIGURE 4.** Results from X-inactivation (XCI) ratio testing with RNA-seq data for nine AIC cases. (A) The XCI ratio for all nine cases. We identified that the AIC case from Fam10 (family 10) has extreme skewed XCI. **Bold line:** 90 XCI cutoff for extreme skewing; **dotted line:** 80 XCI cutoff for moderate skewing. (B) Density plot of the calculated allelic ratio (ratio of reads containing the alternative allele compared to all the reads at the heterozygous locus) and the allelic ratio versus the position on X chromosome in AIC case 10, which demonstrates the extreme skewing of XCI in AIC case 10.

the intestine, the heart, the pituitary gland, the uterus, bronchus, skeletal muscle, and the brain. The highest expression in the brain is in the hippocampus (Supplementary Fig. S5).

In family 7, we identified a de novo variant in *OCELI1* (p.Ala167Thr). The function of *OCELI1* is unknown, but it is highly expressed in the eye and retina and is highly upregulated in retinas in mice exposed to high intraocular pressures.<sup>41</sup> We quantified the expression pattern of *OCELI1* in many tissues, and found that it is also highly expressed in the brain (Supplementary Fig. S5). We consider this variant a candidate for development of AIC in this patient, although the identification of additional patients with mutations in *OCELI1* should confirm the causal relation.

The second part of this study focused on identifying dysregulated pathways/genes that were shared among all AIC cases to identify common pathogenic mechanisms in AIC. This was done by performing RNA-seq on RNA extracted from whole blood from nine AIC cases (not including family 2; *TEAD1*), 15 parents, and 4 age-matched controls (Supplementary Table S1; Fig. 2). We identified several significant genes important either in the retina or in brain development. Of interest is that most of the neuronal genes in our set have previously been reported to be involved in neuronal synaptic plasticity or have been associated with seizures (Fig. 2). Neuronal synaptic plasticity provides the basis for most models of learning, memory, and development in neural circuits<sup>42</sup> and seems to be one of the key components dysregulated in AIC cases (Fig. 2).

Furthermore, infantile spasms is one of the classic features of AIC, sometimes asymmetric or even unilateral.<sup>1</sup> Several genes implicated in other disorders with seizures are dysregulated in AIC cases as well (Fig. 2). Of interest is *HTRA3*, serotonin receptor, which was highly upregulated in four AIC cases (Supplementary Fig. S3) and has been previously found to be upregulated in other syndromes with neonatal seizures.<sup>43</sup> We also found that *GEMIN2* (*SIP1*), which causes Mowat-Wilson syndrome in humans,<sup>44</sup> is upregulated in AIC cases. This syndrome exhibits microcephaly, agenesis of the corpus callosum, cerebral atrophy, and poor hippocampal formation, as well as other non-brain-related congenital defects.<sup>44</sup>

Next, we identified several genes important in eye/retinal development (Fig. 2). Some genes have an important function in both eye and brain and might be of special interest. For example, *PTGS2*, which is significantly downregulated in AIC cases, is a key enzyme in the conversion of arachidonic acid to prostaglandins in brain, and has been implicated in several neurologic disorders, including epilepsy. It is expressed in postsynaptic dendritic spines and is very important in neuronal plasticity.<sup>45</sup> In addition, in the retina, this gene is localized to sites associated with retinal blood vessels, and it plays an important role in blood vessel formation.<sup>46</sup>

These data suggest that dysregulation of neuronal plasticity is an important mechanism in the development AIC, and highlights several genes important in retinal and neuronal development that might contribute to the mechanisms underlying chorioretinal lacunae and infantile spasms. Lastly, since *TEAD1* has an important function in the regulation of cellular growth and apoptosis, we looked at dysregulated genes important in cell cycle control and apoptosis. We found several genes among the 147 genes that are important in cell cycle control ( $n = 18$ ; Fig. 3A) and apoptosis ( $n = 3$ ; Fig. 3B). These changes in neuronal plasticity, retinal development, neuronal development, and apoptosis/cell cycle control are part of the pathogenic mechanisms underlying AIC in these families or be might part of the adaptive responses to the disturbed environment.

Several X-linked disorders have been associated with nonrandom X chromosome (XCI) inactivation in females. Eble et al.<sup>47</sup> reported that there is a significant difference in the occurrence of XCI between patients with AIC and controls, suggesting a mechanism for disease risk. We could demonstrate extreme XCI in one of the nine AIC cases (11%).<sup>47</sup> This confirms that nonrandom XCI might be important in the development of the disease in some cases. In addition, we can suggest that the AIC case of family 10, and possibly also that of family 3, are caused by a mutation on the X chromosome in combination with XCI skewing.

Aicardi syndrome is described almost exclusively in girls or 47, XXY boys. However, some reports have described boys with 46, XY.<sup>11,12</sup> It was speculated by the authors that these cases either were not X linked or were mosaic for mutations in the putative X-linked AIC gene. Our current data suggest that these cases might in fact be caused by a mutation of an autosomal gene with a similar pathogenic mechanism to the gene on the X chromosome, and that AIC is a genetically heterogeneous disease. Genetic heterogeneity in AIC is further supported by two reported cases of AIC, one with a 6q deletion;12q duplication<sup>48</sup> and one with a de novo 11.73-Mb terminal deletion of chr1p36.<sup>49</sup> We suggest that male sex should not exclude the diagnosis of AIC and that the search for mutations causing AIC should include autosomal genes.

In conclusion, we identified a mutation in autosomal gene *TEAD1* in a case diagnosed with AIC, and supporting the involvement of *TEAD1* mutations in several chorioretinal complications. Furthermore, this finding supports the idea that AIC is a genetically heterogeneous disorder with variable phenotypic presentations, and that males with similar features should be considered for diagnosis of AIC. In addition, we were able to identify several important and potentially pathogenic mechanisms shared by AIC cases, including the dysregulation of genes important in neuronal synaptic plasticity and retinal developmental.

### Acknowledgments

IS is a postdoctoral fellow of the FWO-Vlaanderen. The authors alone are responsible for the content and writing of the paper.

Disclosure: **I. Schrauwen**, None; **S. Szelingner**, None; **A.L. Siniard**, None; **J.J. Corneveaux**, None; **A. Kurdoglu**, None; **R. Richholt**, None; **M. De Both**, None; **I. Malenica**, None; **S. Swaminathan**, None; **S. Rangasamy**, None; **N. Kulkarni**, None; **S. Bernes**, None; **J. Buchhalter**, None; **K. Ramsey**, None; **D.W. Craig**, None; **V. Narayanan**, None; **M.J. Huentelman**, None

### References

1. Aicardi J. Aicardi syndrome. *Brain Dev.* 2005;27:164-171.
2. Fruhman G, Eble TN, Gambhir N, Sutton VR, Van den Veyver IB, Lewis RA. Ophthalmologic findings in Aicardi syndrome. *J AAPOS.* 2012;16:238-241.
3. Hoyt CS, Billson F, Ouvrier R. Ocular features of Aicardi's syndrome. *Arch Ophthalmol.* 1978;96:291-295.
4. Menezes AV, Lewis TL, Buncic JR. Role of ocular involvement in the prediction of visual development and clinical prognosis in Aicardi syndrome. *Br J Ophthalmol.* 1996;80:805-811.
5. Kroner BL, Preiss LR, Ardini M-A, Gaillard WD. New incidence, prevalence, and survival of Aicardi syndrome from 408 cases. *J Child Neurol.* 2008;23:531-535.
6. Hopkins IJ, Humphrey I, Keith CG, Susman M, Webb GC, Turner EK. The Aicardi syndrome in a 47, XXY male. *J Paediatr Child Health.* 1979;15:278-280.
7. Zubairi MS, Carter RE, Ronen GM. A male phenotype with Aicardi syndrome. *J Child Neurol.* 2009;24:204-207.

8. Ropers HH, Zuffardi O, Bianchi E, Tiepolo L. Agenesis of corpus callosum, ocular, and skeletal anomalies (X-linked dominant Aicardi's syndrome) in a girl with balanced X/3 translocation. *Hum Genet.* 1982;61:364-368.
9. Donnenfeld AE, Packer RJ, Zackai EH, Chee CM, Sellinger B, Emanuel BS. Clinical, cytogenetic, and pedigree findings in 18 cases of Aicardi syndrome. *Am J Med Genet.* 1989;32:461-467.
10. Thomas GH. High male:female ratio of germ-line mutations: an alternative explanation for postulated gestational lethality in males in X-linked dominant disorders. *Am J Hum Genet.* 1996; 58:1364-1368.
11. Aggarwal KC, Aggarwal A, Prasad MS, Salhan RN, Upadhya A. Aicardi's syndrome in a male child: an unusual presentation. *Indian Pediatr.* 2000;37:542-545.
12. Chappelov AV, Reid J, Parikh S, Traboulsi EI. Aicardi syndrome in a genotypic male. *Ophthalmic Genet.* 2008;29:181-183.
13. Sutton V, Van den Veyver I. *Aicardi Syndrome.* GeneReviews. Seattle, WA: Pagon, RA; 2006.
14. Li H, Durbin R. Fast and accurate long-read alignment with Burrows-Wheeler transform. *Bioinformatics.* 2010;26:589-595.
15. Li H, Handsaker B, Wysoker A, et al. The Sequence Alignment/Map format and SAMtools. *Bioinformatics.* 2009;25:2078-2079.
16. McKenna A, Hanna M, Banks E, et al. The Genome Analysis Toolkit: a MapReduce framework for analyzing next-generation DNA sequencing data. *Genome Res.* 2010;20:1297-1303.
17. Cingolani P, Platts A, Wang LL, et al. A program for annotating and predicting the effects of single nucleotide polymorphisms, SnpEff: SNPs in the genome of *Drosophila melanogaster* strain w1118; iso-2; iso-3. *Fly (Austin).* 2012;6:80-92.
18. Widmann J, Stombaugh J, McDonald D, et al. RNASAR: an RNA STructural Alignment Repository that provides insight into the evolution of natural and artificial RNAs. *RNA.* 2012;18: 1319-1327.
19. Anders S, Pyl PT, Huber W. HTSeq—a Python framework to work with high-throughput sequencing data. *Bioinformatics.* 2015;31:166-169.
20. Anders S, Huber W. Differential expression analysis for sequence count data. *Genome Biol.* 2010;11:R106.
21. Pollier J, Rombauts S, Goossens A. Analysis of RNA-Seq data with TopHat and Cufflinks for genome-wide expression analysis of jasmonate-treated plants and plant cultures. *Methods Mol Biol.* 2013;1011:305-315.
22. Croft D, O'Kelly G, Wu G, et al. Reactome: a database of reactions, pathways and biological processes. *Nucleic Acids Res.* 2011;39(database issue):D691-D697.
23. Chen J, Bardes EE, Aronow BJ, Jegga AG. ToppGene Suite for gene list enrichment analysis and candidate gene prioritization. *Nucleic Acids Res.* 2009;37(web server issue):W305-W311.
24. Kim D, Pertea G, Trapnell C, Pimentel H, Kelley R, Salzberg SL. TopHat2: accurate alignment of transcriptomes in the presence of insertions, deletions and gene fusions. *Genome Biol.* 2013;14:R36.
25. Szelinger S, Malenica I, Corneveaux J, et al. Characterization of X chromosome inactivation using integrated analysis of whole-exome and mRNA sequencing. *PLoS One.* 2014;9:e113036.
26. Busque L, Zhu J, DeHart D, et al. An expression based clonality assay at the human androgen receptor locus (HUMARA) on chromosome X. *Nucleic Acids Res.* 1994;22:697-698.
27. Langmead B, Salzberg SL. Fast gapped-read alignment with Bowtie 2. *Nat Methods.* 2012;9:357-359.
28. Bordes L, Chauveau D, Vandekerckhove P. A stochastic EM algorithm for a semiparametric mixture model. *Comput Stat Data Anal.* 2007;51:5429-5443.
29. Kircher M, Witten DM, Jain P, O'Roak BJ, Cooper GM, Shendure J. A general framework for estimating the relative pathogenicity of human genetic variants. *Nat Genet.* 2014;46:310-315.
30. De la Rosa DA, Krueger SR, Kolar A, Shao D, Fitzsimonds RM, Canessa CM. Distribution, subcellular localization and ontogeny of ASIC1 in the mammalian central nervous system. *J Physiol.* 2002;546:77-87.
31. Kaneko KJ, DePamphilis ML. Regulation of gene expression at the beginning of mammalian development and the TEAD family of transcription factors. *Dev Genet.* 1998;22:43-55.
32. Fossdal R, Jonasson F, Kristjansdottir GT, et al. A novel TEAD1 mutation is the causative allele in Sveinsson's chorioretinal atrophy (helicoid peripapillary chorioretinal degeneration). *Hum Mol Genet.* 2004;13:975-981.
33. Kitagawa M. A Sveinsson's chorioretinal atrophy-associated missense mutation in mouse Tead1 affects its interaction with the co-factors YAP and TAZ. *Biochem Biophys Res Commun.* 2007;361:1022-1026.
34. Landin Malt A, Cagliero J, Legent K, Silber J, Zider A, Flagiello D. Alteration of TEAD1 expression levels confers apoptotic resistance through the transcriptional up-regulation of Livin. *PLoS One.* 2012;7:e45498.
35. Williamson KA, Rainger J, Floyd JAB, et al. Heterozygous loss-of-function mutations in YAP1 cause both isolated and syndromic optic fissure closure defects. *Am J Hum Genet.* 2014;94:295-302.
36. Yu F-X, Guan K-L. The Hippo pathway: regulators and regulations. *Genes Dev.* 2013;27:355-371.
37. Zhao B, Ye X, Yu J, et al. TEAD mediates YAP-dependent gene induction and growth control. *Genes Dev.* 2008;22:1962-1971.
38. Lamar JM, Stern P, Liu H, Schindler JW, Jiang Z-G, Hynes RO. The Hippo pathway target, YAP, promotes metastasis through its TEAD-interaction domain. *Proc Natl Acad Sci U S A.* 2012; 109:E2441-E2450.
39. Landin Malt A, Georges A, Silber J, Zider A, Flagiello D. Interaction with the Yes-associated protein (YAP) allows TEAD1 to positively regulate NAIP expression. *FEBS Lett.* 2013;587:3216-3223.
40. Naye F, Tréguer K, Soulet F, et al. Differential expression of two TEF-1 (TEAD) genes during *Xenopus laevis* development and in response to inducing factors. *Int J Dev Biol.* 2007;51:745-752.
41. Panagis L, Zhao X, Ge Y, Ren L, Mittag TW, Danias J. Retinal gene expression changes related to IOP exposure and axonal loss in DBA/2J mice. *Invest Ophthalmol Vis Sci.* 2011;52: 7807-7816.
42. Abbott LF, Nelson SB. Synaptic plasticity: taming the beast. *Nat Neurosci.* 2000;3(suppl):1178-1183.
43. Kaya N, Imtiaz F, Colak D, et al. Genome-wide gene expression profiling and mutation analysis of Saudi patients with Canavan disease. *Genet Med.* 2008;10:675-684.
44. Mowat DR. Mowat-Wilson syndrome. *J Med Genet.* 2003;40: 305-310.
45. Chen C, Magee JC, Bazan NG. Cyclooxygenase-2 regulates prostaglandin E2 signaling in hippocampal long-term synaptic plasticity. *J Neurophysiol.* 2002;87:2851-2857.
46. Wilkinson-Berka JL. COX-2 inhibition and retinal angiogenesis in a mouse model of retinopathy of prematurity. *Invest Ophthalmol Vis Sci.* 2003;44:974-979.
47. Eble TN, Sutton VR, Sangi-Haghpeykar H, et al. Non-random X chromosome inactivation in Aicardi syndrome. *Hum Genet.* 2009;125:211-216.
48. Prontera P, Bartocci A, Ottaviani V, et al. Aicardi syndrome associated with autosomal genomic imbalance: coincidence or evidence for autosomal inheritance with sex-limited expression? *Mol Syndromol.* 2013;4:197-202.
49. Bursztejn A-C, Bronner M, Peudenier S, Grégoire M-J, Jonveaux P, Nemos C. Molecular characterization of a monosomy 1p36 presenting as an Aicardi syndrome phenocopy. *Am J Med Genet A.* 2009;149A:2493-2500.